

Testing Lorentz Invariance using Zeeman Transitions in Atomic Fountains

Peter Wolf

SYRTE, Observatoire de Paris

and

Bureau International des Poids et Mesures

Pavillon de Breteuil, 92312 Sèvres, Cedex, France

Frédéric Chapelet

Sébastien Bize

André Clairon

SYRTE, Observatoire de Paris

61 av. de l'Observatoire, 75014 Paris, France

Abstract— Lorentz Invariance (LI) is the founding postulate of Einstein's 1905 theory of relativity, and therefore at the heart of all accepted theories of physics. It characterizes the invariance of the laws of physics in inertial frames under changes of velocity or orientation. This central role, and indications from unification theories [1], [2], [3] hinting toward a possible LI violation, have motivated tremendous experimental efforts to test LI. A comprehensive theoretical framework to describe violations of LI has been developed over the last decade [4]: the Lorentz violating Standard Model Extension (SME). It allows a characterization of LI violations in all fields of present day physics using a large (but finite) set of parameters which are all zero when LI is satisfied. All classical tests (e.g. Michelson-Morley or Kennedy-Thorndike experiments [5], [6]) can be analyzed in the SME, but it also allows the conception of new types of experiments, not thought of previously. We have carried out such a conceptually new LI test, by comparing particular atomic transitions (particular orientations of the involved nuclear spins) in the ^{133}Cs atom using a cold atomic fountain clock. This allows us to test LI in a previously largely unexplored region of the SME parameter space, corresponding to first measurements of four proton parameters and an improvement by 11 and 12 orders of magnitude on the determination of four others. In spite of the attained accuracies, and of having extended the search into a new region of the SME, we still find no indication of LI violation.

The experiment reported here tests for a violation of LI by searching for a variation of atomic transition frequencies as a function of the orientation of the spin of the involved atomic states (clock comparison or Hughes-Drever experiment). Based on the SME analysis of numerous atomic transitions in [7], [8] we have chosen the measurement of a particular combination of transitions in the ^{133}Cs atom. This provides good sensitivity to the quadrupolar SME energy shift of the proton (as defined in [7]) in the spin $\frac{7}{2}$ Cs nucleus, whilst being largely insensitive to magnetic perturbations (first order Zeeman effect). The corresponding region of the SME parameter space has been largely unexplored previously, with first limits on some parameters set only very recently [9] by a re-analysis of the Doppler spectroscopy experiment (Ives-Stilwell experiment) of [10]. Given the large improvement (11 and 12 orders of magnitude on four parameters) we obtain with respect to those results, and the qualitatively new region explored (first measurements of four parame-

ters), the experiment had comparatively high probability for the detection of a positive Lorentz violating signal. However, our results clearly exclude that possibility.

The SME was developed relatively recently by Kostelecký and co-workers [4], motivated initially by possible Lorentz violating phenomenological effects of string theory [1]. It consists of a parameterized version of the standard model Lagrangian that includes all Lorentz violating terms that can be formed from known fields, and includes (in its most recent version) gravity. In its minimal form the SME characterizes Lorentz violation in the matter sector by 44 parameters per particle [7], [8], of which 40 are accessible to terrestrial experiments at first order in v_{\oplus}/c [8] (v_{\oplus} is the orbital velocity of the Earth and $c = 299792458$ m/s). All SME parameters vanish when LI is verified. Existing bounds for the proton (p^+), neutron (n) and electron (e^-) come from clock comparison and magnetometer experiments using different atomic species (see [7] and references therein, [11], [12], [13], [14]), from resonator experiments [15], [6], [16], and from Ives-Stilwell experiments [9], [10]. They are summarized in tab. I, together with the results reported in this work.

For our experiment we use one of the laser cooled fountain clocks operated at the Paris observatory, the ^{133}Cs and ^{87}Rb double fountain FO2 (see [17] for a detailed description). We run it in Cs mode on the $|F = 3\rangle \leftrightarrow |F = 4\rangle$ hyperfine transition of the $6S_{1/2}$ ground state. Both hyperfine states are split into Zeeman substates $m_F = [-3, 3]$ and $m_F = [-4, 4]$ respectively. The clock transition used in routine operation is $|F = 3, m_F = 0\rangle \leftrightarrow |F = 4, m_F = 0\rangle$ at 9.2 GHz, which is magnetic field independent to first order. The first order magnetic field dependent Zeeman transitions ($|3, i\rangle \leftrightarrow |4, i\rangle$ with $i = \pm 1, \pm 2, \pm 3$) are used regularly for measurement and characterization of the magnetic field, necessary to correct the second order Zeeman effect of the clock transition. In routine operation the clock transition frequency stability of FO2 is $1.6 \times 10^{-14} \tau^{-1/2}$, and its accuracy 7×10^{-16} [17], [18].

A detailed description of the minimal SME as applied to the perturbation of atomic energy levels and transition frequencies can be found in [7], [8]. Based on the Schmidt

TABLE I

Orders of magnitude of present limits (in GeV) on Lorentz violating parameters in the minimal SME matter sector and corresponding references. Indices J, K run over X, Y, Z with $J \neq K$. Limits from the present work are in bold type, with previous limits (when available) in brackets.

Parameter	p ⁺	n	e ⁻	Ref.
\tilde{b}_X, \tilde{b}_Y	10^{-27}	10^{-31}	10^{-29}	[11], [12], [13]
\tilde{b}_Z	-	-	10^{-28}	[13]
$\tilde{b}_T, \tilde{g}_T, H_{JT}, \tilde{d}_{\pm}$	-	10^{-27}	-	[14]
$\tilde{d}_Q, \tilde{d}_{XY}, \tilde{d}_{YZ}$	-	10^{-27}	-	[14]
\tilde{d}_X, \tilde{d}_Y	10^{-25}	10^{-29}	10^{-22}	[7], [14], [7]
$\tilde{d}_{XZ}, \tilde{d}_Z$	-	-	-	
$\tilde{g}_{DX}, \tilde{g}_{DY}$	10^{-25}	10^{-29}	10^{-22}	[7], [14], [7]
$\tilde{g}_{DZ}, \tilde{g}_{JK}$	-	-	-	
\tilde{g}_c	-	10^{-27}	-	[14]
$\tilde{g}_-, \tilde{g}_Q, \tilde{g}_{TJ}$	-	-	-	
\tilde{c}_Q	$10^{-22}(-11)$	-	10^{-9}	[9], [10]
\tilde{c}_X, \tilde{c}_Y	10^{-24}	10^{-25}	10^{-19}	[7], [15], [6], [16]
\tilde{c}_Z, \tilde{c}_-	10^{-24}	10^{-27}	10^{-19}	[7], [15], [6], [16]
\tilde{c}_{TJ}	$10^{-20}(-8)$	-	10^{-6}	[9], [10]

nuclear model¹ one can derive the SME frequency shift of a Cs $|3, m_F\rangle \leftrightarrow |4, m_F\rangle$ transition in the form

$$\begin{aligned} \delta\nu = & \frac{m_F}{14h} \left(\beta_p \tilde{b}_3^p - \delta_p \tilde{d}_3^p + \kappa_p \tilde{g}_d^p \right) - \frac{m_F^2}{14h} (\gamma_p \tilde{c}_q^p) \\ & - \frac{m_F}{2h} \left(\beta_e \tilde{b}_3^e - \delta_e \tilde{d}_3^e + \kappa_e \tilde{g}_d^e \right) \\ & + m_F K_Z^{(1)} B + \left(1 - \frac{m_F^2}{16} \right) K_Z^{(2)} B^2 \end{aligned} \quad (1)$$

for the quantization magnetic field in the negative z direction (vertically downward) in the lab frame. The first three terms in (1) are Lorentz violating SME frequency shifts, the last two describe the first and second order Zeeman frequency shift (we neglect B^3 and higher order terms). The tilde quantities are linear combinations of the SME matter sector parameters of tab. I in the lab frame, with p,e standing for the proton and electron respectively. The quantities $\beta_w, \delta_w, \kappa_w, \gamma_w, \lambda_w$ (with $w = p, e$) depend on the nuclear and electronic structure, they are given in tab. II of [8], h is Planck's constant, B is the magnetic field seen by the atom, $K_Z^{(1)} = 7.008 \text{ Hz nT}^{-1}$ is the first order Zeeman coefficient, $K_Z^{(2)} = 427.45 \times 10^8 \text{ Hz T}^{-2}$ is the second order coefficient [19]. The tilde quantities in (1) are time varying due to the motion of the lab frame (and hence the quantization field) in a cosmological frame, inducing modulations of the frequency shift at sidereal and semi-sidereal frequencies, which can be searched for.

From (1) we note that the $m_F = 0$ clock transition is insensitive to Lorentz violation or the first order Zeeman shift, while the Zeeman transitions ($m_F \neq 0$) are sensitive

¹As discussed in [7] the Schmidt nuclear model only allows an approximate calculation of the SME frequency shift, with more complex models generally leading to dependences on additional SME parameters. Nonetheless, the model is sufficient to derive the leading order terms and has been used for the analysis of most experiments providing the bounds in Tab. I.

to both. Hence, a direct measurement of a Zeeman transition with respect to the clock transition allows a LI test. However, such an experiment would be severely limited by the strong dependence of the Zeeman transition frequency on B , and its diurnal and semi-diurnal variations. To avoid such a limitation, we "simultaneously" (see below) measure the $m_F = 3$, $m_F = -3$ and $m_F = 0$ transitions and form the combined observable $\nu_c \equiv \nu_{+3} + \nu_{-3} - 2\nu_0$. From (1)

$$\nu_c = \frac{1}{7h} K_p \tilde{c}_q^p - \frac{9}{8} K_Z^{(2)} B^2 \quad (2)$$

where we have used $\gamma_p = -K_p/9$ from [8] ($K_p \sim 10^{-2}$ in the Schmidt nuclear model). This observable is insensitive to the first order Zeeman shift, and should be zero up to the second order Zeeman correction and a possible Lorentz violating shift in the first term of (2).

The lab frame parameter \tilde{c}_q^p can be related to the conventional sun-centered frame parameters of the SME (the parameters of tab. I) by a time dependent boost and rotation (see [8] for details). This leads to a general expression for the observable ν_c of the form

$$\begin{aligned} \nu_c = A & + C_{\omega_\oplus} \cos(\omega_\oplus T_\oplus) + S_{\omega_\oplus} \sin(\omega_\oplus T_\oplus) \\ & + C_{2\omega_\oplus} \cos(2\omega_\oplus T_\oplus) + S_{2\omega_\oplus} \sin(2\omega_\oplus T_\oplus), \end{aligned} \quad (3)$$

where ω_\oplus is the frequency of rotation of the Earth, T_\oplus is time since 30 March 2005 11h 19min 25s UTC (consistent with the definitions in [20]), and with $A, C_{\omega_\oplus}, S_{\omega_\oplus}, C_{2\omega_\oplus}$ and $S_{2\omega_\oplus}$ given in tab. II as functions of the sun frame SME parameters. A least squares fit of (3) to our data provides the measured values given in tab. II, and the corresponding determination of the SME parameters.

The FO2 setup is sketched in fig. 1. Cs atoms effusing from an oven are slowed using a chirped counter propagating laser beam and captured in a lin \perp lin optical molasses. Atoms are cooled by six laser beams supplied by pre

TABLE II

Coefficients of (3) to first order in $\beta \equiv v_{\oplus}/c$, where Ω_{\oplus} is the angular frequency of the Earth's orbital motion, T is time since the March equinox, $\chi = 41.2^\circ$ is the colatitude of our lab, and $\eta = 23.3^\circ$ is the inclination of the Earth's orbit. The measured values (in mHz) are shown together with the statistical (first bracket) and systematic (second bracket) uncertainties. For our relatively short data set (21 days) we neglect the slow variation due to the annual terms and take $\Omega_{\oplus}T \sim 0.34$ rad.

A	$\frac{K_p}{28h} (1 + 3\cos(2\chi)) (\tilde{c}_Q + \beta(\sin(\Omega_{\oplus}T)\tilde{c}_{TX} + \cos(\Omega_{\oplus}T)(2\sin\eta\tilde{c}_{TZ} - \cos\eta\tilde{c}_{TY})) - \frac{9}{8}K_Z^{(2)}B^2$	-5.7(0.05)(26)
$C_{\omega_{\oplus}}$	$-\frac{3K_p}{14h}\sin(2\chi)(\tilde{c}_Y + \beta(\sin(\Omega_{\oplus}T)\tilde{c}_{TZ} - \cos(\Omega_{\oplus}T)\sin\eta\tilde{c}_{TX}))$	0.1(0.07)(0.35)
$S_{\omega_{\oplus}}$	$-\frac{3K_p}{14h}\sin(2\chi)(\tilde{c}_X - \beta\cos(\Omega_{\oplus}T)(\sin\eta\tilde{c}_{TY} + \cos\eta\tilde{c}_{TZ}))$	-0.03(0.07)(0.35)
$C_{2\omega_{\oplus}}$	$-\frac{3K_p}{14h}\sin^2\chi(\tilde{c}_- + \beta(\sin(\Omega_{\oplus}T)\tilde{c}_{TX} + \cos(\Omega_{\oplus}T)\cos\eta\tilde{c}_{TY}))$	0.04(0.07)(0.35)
$S_{2\omega_{\oplus}}$	$-\frac{3K_p}{14h}\sin^2\chi(\tilde{c}_Z + \beta(\sin(\Omega_{\oplus}T)\tilde{c}_{TY} - \cos(\Omega_{\oplus}T)\cos\eta\tilde{c}_{TX}))$	-0.02(0.07)(0.35)

adjusted optical fiber couplers precisely attached to the vacuum tank and aligned along the axes of a 3 dimensional coordinate system, where the (111) direction is vertical. Compared to typical FO2 clock operation [17], the number of atoms loaded in the optical molasses has been reduced to 2×10^7 atoms captured in 30 ms. This reduces the collisional frequency shift of ν_c to below 0.1 mHz, and even less for its variation at ω_{\oplus} and $2\omega_{\oplus}$.

Atoms are launched upwards at 3.94 m.s⁻¹ by using a moving optical molasses and cooled to $\sim 1 \mu\text{K}$ in the moving frame by adiabatically decreasing the laser intensity and increasing the laser detuning. Atoms are then selected by means of a microwave excitation in the selection cavity performed in a bias magnetic field of $\sim 20 \mu\text{T}$, and of a push laser beam. Any of the $|3, m_F\rangle$ states can be prepared with a high degree of purity (few 10^{-3}) by tuning the selection microwave frequency. 52 cm above the capture zone, a cylindrical copper cavity (TE₀₁₁ mode) is used to probe the $|3, m_F\rangle \leftrightarrow |4, m_F\rangle$ hyperfine transition at 9.2 GHz. The Ramsey interrogation method is performed by letting the atomic cloud interact with the microwave field a first time on the way up and a second time on the way down. After the interrogation, the populations $N_{F=4}$ and $N_{F=3}$ of the two hyperfine levels are measured by laser induced fluorescence, leading to a determination of the transition probability $P = N_3/(N_3 + N_4)$ which is insensitive to atom number fluctuations. One complete fountain cycle from capture to detection lasts 1045 ms in the present experiment. From the transition probability, measured on both sides of the central Ramsey fringe, we compute an error signal to lock the microwave interrogation frequency to the atomic transition using a digital servo loop. The frequency corrections are applied to a computer controlled high resolution DDS synthesizer in the microwave generator. These corrections are used to measure the atomic transition frequency with respect to the local reference signal used to synthesize the microwave frequency.

The homogeneity and the stability of the magnetic field in the interrogation region is a crucial point for the experiment. A magnetic field of 203 nT is produced by a main solenoid (length 815 mm, diameter 220 mm) and

a set of 4 compensation coils. These coils are surrounded by a first layer of 3 cylindrical magnetic shields. A second layer is composed of 2 magnetic shields surrounding the entire experiment (optical molasses and detection zone included). Between the two layers, the magnetic field fluctuations are sensed with a flux-gate magnetometer and stabilized by acting on 4 hexagonal coils. The magnetic field in the interrogation region is probed using the $|3, 1\rangle \leftrightarrow |4, 1\rangle$ atomic transition. Measurements of the transition frequency as a function of the launch height show a peak to peak spatial dependence of 230 pT over a range of 320 mm above the interrogation cavity with a variation of $\leq 0.1 \text{ pT/mm}$ around the apogee of the atomic trajectories. Measurements of the same transition as a function of time at the launch height of 791 mm show a magnetic field instability near 2 pT for an integration time of $\tau = 1 \text{ s}$. The long term behavior exhibits residual variations of the magnetic field ($\sim 0.7 \text{ pT}$ at $\tau = 10000 \text{ s}$) induced by temperature fluctuations which could cause variations of the current flowing through solenoid, of the solenoid geometry, of residual thermoelectric currents, of the magnetic shield permeability, etc...

The experimental sequence is tailored to circumvent the limitation that the long term magnetic field fluctuations could cause. First $|3, -3\rangle$ atoms are selected and the $|3, -3\rangle \leftrightarrow |4, -3\rangle$ transition is probed at half maximum on the red side of the resonance (0.528 Hz below the resonance center). The next fountain cycle, $|3, +3\rangle$ atoms are selected and the $|3, +3\rangle \leftrightarrow |4, +3\rangle$ transition is also probed at half maximum on the red side of the resonance. The third and fourth fountain cycles, the same two transitions are probed on the blue side of the resonances (0.528 Hz above the resonance centers). This 4180 ms long sequence is repeated so as to implement two interleaved digital servo loops finding the line centers of both the $|3, -3\rangle \leftrightarrow |4, -3\rangle$ and the $|3, +3\rangle \leftrightarrow |4, +3\rangle$ transitions. Every 400 fountain cycles, the above sequence is interrupted and the regular clock transition $|3, 0\rangle \leftrightarrow |4, 0\rangle$ is measured for 10 s allowing for an absolute calibration of the local frequency reference with a suitable statistical uncertainty. Using this sequence, magnetic field fluctuations over timescales $\geq 4 \text{ s}$ are rejected in the combined observable ν_c and the stability

is dominated by the short term ($\tau < 4$ s) magnetic field fluctuations.

We have taken data implementing the experimental sequence described above over a period of 21 days starting on march 30, 2005. The complete raw data (no post-treatment) is shown in fig. 2, each point representing a ~ 432 s measurement sequence of $\nu_{+3} + \nu_{-3} - 2\nu_0$ as described above. The inset in fig. 2 shows the frequency stability of the last continuous stretch of data (~ 10 days). We note the essentially white noise behavior of the data on that figure, indicating that the experimental sequence successfully rejects all long term variations of the magnetic field or of other perturbing effects. A least squares fit of the model (3) to the complete data provides the 5 coefficients and statistical uncertainties given in tab. II.

We note a statistically significant offset of the data from zero ($-5.7(0.05)$ mHz). This is partly due to the second order Zeeman shift (second term in (2)) which amounts to -2.0 mHz. The remaining -3.7 mHz are either due to a systematic effect or indicate a genuine Lorentz violating signal.

The dominant systematic effect in our experiment is most likely a residual first order Zeeman shift. This arises when the $m_F = -3$ and $m_F = +3$ atoms have slightly different trajectories in the presence of a magnetic field gradient. The result is a difference in first order Zeeman shift and hence incomplete cancelation in the combined observable ν_c . To test this hypothesis we have taken 3 hours of time of flight (TOF) measurements of the atoms in the different Zeeman states. We observe a significant TOF difference of $155\ \mu\text{s}$ (when launching at $4.25\ \text{m/s}$) between the $m_F = -3$ and $m_F = +3$ states, most likely due to slight magnetic and optical differences in the laser trapping and cooling during the final adiabatic phase.

We model a residual first order Zeeman effect using a Monte Carlo (MC) simulation with the measured vertical magnetic field map, and assuming that the complete TOF

difference is due to an initial vertical spatial offset ($\sim 660\ \mu\text{m}$) between the atoms rather than an offset in launch velocity. In this scenario, which maximizes the resulting frequency shift, we obtain a frequency offset of only $\sim 5\ \mu\text{Hz}$ in ν_c .

Another indication for magnetic field inhomogeneities comes from measurements of the contrast of the Ramsey fringes for the different Zeeman transitions. The measured contrasts are 0.94, 0.93, 0.87, and 0.75 for the $m_F = +0$, $m_F = +1$, $m_F = +2$, and $m_F = +3$ transitions respectively. The observed differences cannot be explained by the known vertical magnetic field gradient alone, but are due to an additional horizontal field gradient, probably caused by residual magnetization inside the magnetic shields or lack of symmetry in the shielding or compensation. Our MC simulation reproduces the measured contrasts when we include a constant horizontal gradient of $\sim 6\ \text{pT/mm}$. To check this value we have slightly tilted the fountain (by up to $\sim 1800\ \mu\text{rad}$ off the vertical) and measured the corresponding change in frequency of the $m_F = +1$ Zeeman transition. The obtained field gradient is somewhat smaller ($\sim 2\ \text{pT/mm}$) but we consider the latter method less accurate, and conservatively use the larger value obtained from the contrast measurements.

Including the thus determined horizontal field gradient in a complete MC simulation we obtain a total offset in ν_c of ~ 26 mHz, assuming that the horizontal spatial offset between the $m_F = -3$ and $m_F = +3$ atoms is identical to the measured vertical offset ($660\ \mu\text{m}$). We consider this to be an upper limit (the horizontal separation is likely to be less than the vertical one due to the absence of gravity), and take it as the systematic uncertainty on the determined offset (A in tab. II).

To determine the systematic uncertainty on the sidereal and semi-sidereal modulations of ν_c we have measured the variation of the $m_F = 0$ TOF at those frequencies and taken the result as the maximum variation of the $m_F = +3$ vs $m_F = -3$ TOF difference (note that the real value is

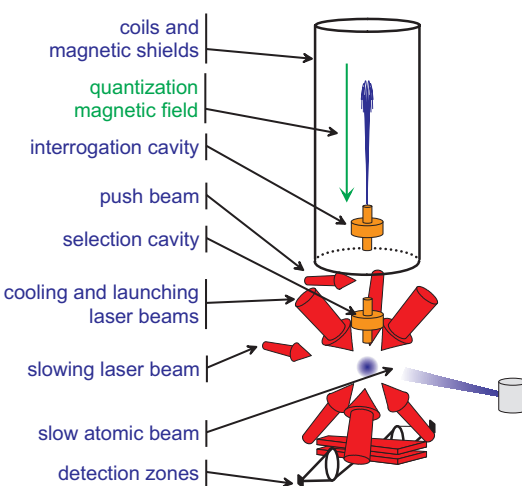


Fig. 1. Schematic view of an atomic fountain.

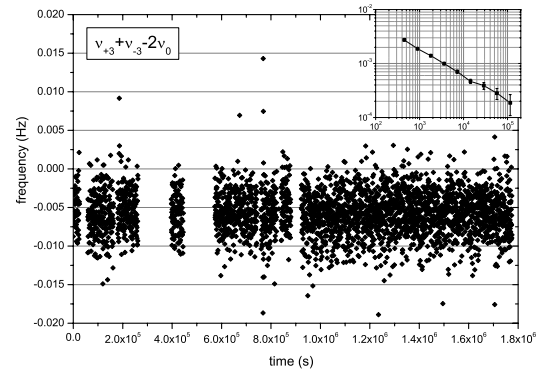


Fig. 2. Raw data of the measurements of $(\nu_{+3} + \nu_{-3} - 2\nu_0)$ spanning ~ 21 days. The inset shows the stability (standard deviation) of the last continuous stretch of data (~ 10 days).

TABLE III

Results for SME Lorentz violating parameters \tilde{c} for the proton, in GeV and with $J = X, Y, Z$.

$\tilde{c}_Q = -0.3(2.2) \times 10^{-23}$	$\tilde{c}_- = -0.2(1.6) \times 10^{-24}$
$\tilde{c}_J = (0.06(0.7), -0.2(0.7), 0.1(1.6)) \times 10^{-24}$	
$\tilde{c}_{TJ} = (0.1(1.3), -0.04(1.7), -0.1(1.0)) \times 10^{-20}$	

probably smaller, due to common mode variations). The best fit amplitudes of the sidereal and semi-sidereal TOF variation are $3.0 \mu\text{s}$ and $2.9 \mu\text{s}$ respectively, which leads to an upper limit of 0.35 mHz on the systematic uncertainties of $C_{\omega_\oplus}, S_{\omega_\oplus}, C_{2\omega_\oplus}, S_{2\omega_\oplus}$ in tab. II.

Finally we use the five measurements and the relations in tab. II to determine the values of the eight SME parameters. In doing so, we assume that there is no correlation between the three \tilde{c}_{TJ} parameters and the other five parameters, and determine them independently. The results are given in tab. III.

In conclusion, we have carried out a test of Lorentz invariance in the matter sector of the minimal SME using Zeeman transition in a cold ^{133}Cs atomic fountain clock. We see no indication of a violation of LI at the present level of experimental uncertainty. Using a particular combination of the different atomic transitions we have set first limits on four proton SME parameters and improved previous limits [9] on four others by 11 and 12 orders of magnitude.

Continuing the experiment regularly over a year or more will allow statistical decorrelation of the three \tilde{c}_{TJ} parameters from the other five, due to their modulation at the annual frequency ($\Omega_\oplus T$ terms in tab. II). Further improvements, and new measurements, could come from the unique capability of our fountain clock to run on ^{87}Rb and ^{133}Cs simultaneously. The different sensitivity of the two atomic species to Lorentz violation (see [8]) and magnetic fields, should allow a measurement of all SME parameters in (1) in spite of the presence of the first order Zeeman effect. Ultimately, space clocks, like the planned ACES mission [21] will provide the possibility of carrying out similar experiments but with faster (90 min orbital period) modulation of the putative Lorentz violating signal, and correspondingly faster data integration.

References

- [1] Kostelecký V.A., Samuel S., Phys.Rev.D39, 683, (1989).
- [2] Damour T., gr-qc/9711060 (1997).
- [3] Gambini R., Pullin J., Phys. Rev. D59, 124021, (1999).
- [4] Colladay D., Kostelecký V.A., Phys.Rev.D55, 6760, (1997); Colladay D., Kostelecký V.A., Phys.Rev.D58, 116002, (1998); Kostelecký V.A., Phys.Rev.D69, 105009, (2004).
- [5] Stanwick P.E., et al., Phys. Rev. Lett. 95, 040404, (2005).
- [6] Wolf P., et al., Phys. Rev. D70, 051902(R), Rapid Communication, (2004).
- [7] Kostelecký V.A., Lane C.D., Phys.Rev.D60, 116010, (1999).
- [8] Bluhm R., et al., Phys. Rev. D68, 125008, (2003).
- [9] Lane C.D., Phys. Rev. D72, 016005, (2005).
- [10] Saathoff G., et al., Phys. Rev. Lett. 91, 19, 190403, (2003).
- [11] Phillips D.F. et al., Phys. Rev. D63, 111101(R), (2001); Humphrey M.A., arXiv:physics/0103068; Phys. Rev. A62, 063405, (2000).
- [12] Bear D. et al., Phys. Rev. Lett. 85, 5038, (2000).
- [13] Hou L.-S., Ni W.-T., Li Y.-C.M., Phys. Rev. Lett. 90, 201101, (2003); Bluhm R. and Kostelecký V.A., Phys. Rev. Lett. 84, 1381, (2000).
- [14] Cané F. et al., Phys. Rev. Lett. 93, 230801, (2004).
- [15] Müller H., Phys. Rev. D71, 045004, (2005).
- [16] Müller H. et al., Phys. Rev. Lett. 91, 2, 020401, (2003).
- [17] Bize S., et al., J. Phys. B38, S449S468, (2005).
- [18] Marion H., et al., Phys. Rev. Lett. 90, 150801, (2003).
- [19] Vanier J., Audoin C., The Quantum Physics of Atomic Frequency Standards, Adam Hilger, (1989).
- [20] Kostelecký A.V. and Mewes M., Phys. Rev. D66, 056005, (2002).
- [21] Salomon C., et al., C.R. Acad. Sci. Paris, 2, 4, 1313, (2001).